Low-Parametric-Crosstalk Phase-Sensitive Amplifier for Guard-Band-Less DWDM Signal Using PPLN Waveguides

Takushi Kazama, Takeshi Umeki, Masashi Abe, Koji Enbutsu, Yutaka Miyamoto, *Member, IEEE*, and Hirokazu Takenouchi, *Member, IEEE*

(Top-scored)

***Abstract*—We demonstrated guard-band-less dense wavelength division multiplex signal amplification with a phase sensitive amplifier (PSA). The PSA consists of periodically poled lithium niobate waveguide that employs two-stage nonlinear process, namely second-harmonic generation and optical parametric amplification, which makes it possible to mitigate the crosstalk induced by the optical parametric interaction between DWDM channels. The PSA amplified 16-channel signals simultaneously with a gain of 17 dB over 12-nm wavelength range. We demonstrated a 2.5-dB signal-to-noise-ratio improvement and a low noise figure of 2.1 dB below the 3-dB quantum limit. We achieved the amplification of a 10-Gbaud quadrature phase shift keying signal with phase and amplitude regeneration.**

***Index Terms*—Nonlinear optics, optical frequency conversion, parametric amplification.**

I. Introduction

ULTRA-DENSE multi-channel transmissions at higher speed will be required for the high capacity optical networks of the future. The signal to noise ratio (SNR) is an essential quantity in terms of achieving greater capacity in a finite bandwidth [1]. To enhance the SNR of optical communication systems, low-noise amplifiers will be needed for broadband multi-channel signals because the excess noise generated by optical amplifiers greatly affects the total amount of noise in the system. Phase-sensitive amplifiers (PSAs) are attracting a lot of interest because they have the potential for low noise amplification while breaking the 3-dB quantum limit on the noise figure (NF) of conventional phase insensitive amplifiers (PIAs) [2] and the signal regeneration capability [3].

Manuscript received June 15, 2016; revised August 19, 2016; accepted August 19, 2016. Date of publication August 30, 2016; date of current version February 22, 2017.

T. Kazama, M. Abe, and K. Enbutsu are with the NTT Device Technology Laboratories, NTT Corporation, Atsugi-shi 243-0198, Japan (e-mail: kazama.takushi@lab.ntt.co.jp; abe.masashi@lab.ntt.co.jp; enbutsu.koji@lab.ntt.co.jp).

T. Umeki and H. Takenouchi are with the NTT Device Technology Laboratories, NTT Corporation, Atsugi-shi 243-0198, Japan, and also with the NTT Network Innovation Labs, NTT Corporation, Yokosuka 239-0847, Japan (e-mail: umeki.takeshi@lab.ntt.co.jp; takenouchi.hirokazu@lab.ntt.co.jp).

Y. Miyamoto is with NTT Network Innovation Labs., NTT Corporation, Yokosuka 239-0847, Japan (e-mail: miyamoto.yutaka@lab.ntt.co.jp).

Color versions of one or more of the figures in this paper are available online at http://ieeexplore.ieee.org.

Digital Object Identifier 10.1109/JLT.2016.2603186

PSAs with two types of parametric processes have been investigated, namely frequency-degenerate (identical signal and idler frequencies) [4], [5] and non-degenerate (different signal and idler frequencies) [6], [7] PSAs. A degenerate PSA only amplifies a single channel signal for a fixed pump configuration. In contrast, the non-degenerate parametric process supports simultaneous multi-channel amplification, which makes it compatible with dense wavelength-division multiplexed (DWDM) systems. The simultaneous amplification of DWDM signals has been demonstrated using both $\chi^{(3)}$-based four-wave mixing [8] and $\chi^{(2)}$-based cascaded second-harmonic generation (SHG) and optical parametric amplification (OPA) [9] processes based on non-degenerate parametric amplification with a phase-conjugated idler. The minimum NF of non-degenerate PSAs is -3 dB when we consider the signal and idler separately [10], [11] (the minimum combined NF is 0 dB when we consider the signal and idler together as the amplifier input and output [12], [13]). As well as having a low noise property, non-degenerate PSAs are known to be capable of improving the SNR of optical links by 3 dB compared with phase-insensitive amplifier links. Tong *et al*. demonstrated these advantages in a non-degenerate PSA with 3-channel WDM signals [14].

The next challenge that we face as regards PSAs is to scale the number of WDM signals without reducing the finite bandwidth and thus apply PSAs to spectrally efficient DWDM signal transmission systems. However, the crosstalk (XT) induced by the optical parametric process itself and the guard band used for mitigating the XT impose a limit on the number of amplifiable WDM channels and the available signal bandwidth. The XT is caused by additionally induced frequency conversion from other WDM signals, which is triggered from the pump generation by a nonlinear interaction between pump-signal, signal-idler and the signal (or idler) itself. Although it has been revealed numerically that the XT is smaller in cascaded $\chi^{(2)}$-based PSAs than in $\chi^{(3)}$-based PSAs thanks to the finite width of the phase-matching band of a $\chi^{(2)}$ nonlinear medium [15], a wide guard band is required because a high power 1.5-μm-band pump generates intense XT components around the pump wavelength that degrade the signal quality. We have already proposed a 2-stage SHG/OPA-based PSA that can eliminate a 1.5-μm-band pump [5]. The configuration has the potential for low-XT parametric

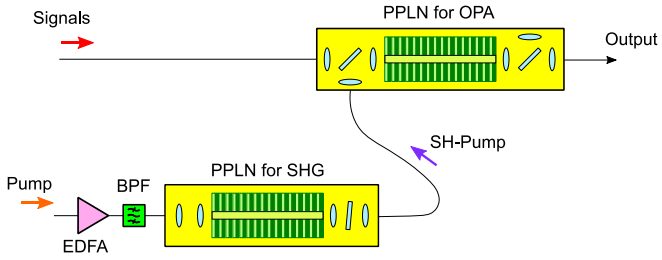

Fig. 1. Configuration of 2-stage SHG/OPA-based PSA. PPLN: periodically poled lithium niobate, SHG: second harmonic generation, OPA: optical parametric amplification, BPF: optical bandpass filter, EDFA: Er-doped fiber amplifier.

amplification. Recently, we demonstrated the low-noise simultaneous phase sensitive amplification of 16-channel DWDM signals thanks to the use of our XT-tolerant 2-stage configuration [16].

In this paper, we describe the XT characteristics of a 2-stage SHG/OPA-based PSA and demonstrate the low-noise simultaneous amplification of guard-band-less DWDM signals. This paper is organized as follows. In Section II, we describe the configuration of a PSA that can suppress the XT generation related to the strong telecom band pump. We show estimation results for unwanted frequency conversion in the PSA. In Section III, we demonstrate the low-XT simultaneous phase sensitive amplification of guard-band-less DWDM CW-signals over a 12-nm wavelength range using the 2-stage SHG/OPA configuration. In Section IV, we describe the noise reduction property and intrinsic NF of the PSA. The PSA provides a 3-dB link SNR advantage over an EDFA and a low NF below the 3-dB quantum limit. Section V describes the amplification of data signals. We demonstrate the amplification of 10-Gbaud quadrature phase shift keying (QPSK) signals with phase and amplitude regeneration.

II. Crosstalk-Tolerant 2-Stage $\chi^{(2)}$ Based PSA and Estimation of Crosstalk

Parametric XT lights are generated by unwanted nonlinear frequency conversion from other WDM channels. A nonlinear interaction between pump-signal, signal-idler, and the signal (or idler) itself generates an undesired pump that induces unwanted frequency conversion. The parametric XT in PSAs can be classified into two types: with and without the participation of a strong telecom-band pump in the XT generation process. Specifically, a strong-pump-related unwanted frequency conversion process generates intense XT components around the pump wavelength, which requires an empty channel band (guard band) between the pump channel and signal band to mitigate the signal quality degradation. The 2-stage SHG/OPA configuration we proposed can suppress both types of XT. Fig. 1 shows the configuration of our 2-stage SHG/OPA-based PSA, which uses two PPLN waveguides based on the direct bonding technique [17]. Each of the 50-mm-long PPLN waveguides is packaged in a module with fiber pigtails. The pump wave is amplified by an EDFA and input into a PPLN module for SHG. Second-harmonic (SH)-pump and signals are input into another PPLN module for OPA.

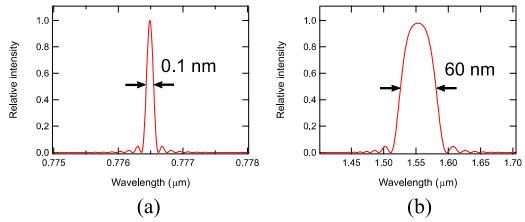

Fig. 2. Calculated phase matching curves. (a) SHG spectrum. (b) DFG spectrum.

To isolate the unwanted amplified spontaneous emission (ASE) around the pump wavelength, an optical band pass filter with a 1 nm bandwidth was inserted between the EDFA and PPLN module for SHG in some experiments. The generated SH-pump was injected into the PPLN module for OPA. The dichroic mirrors in the module effectively suppressed the unwanted output of the 1.5-μm-band pump and ASE generated by the EDFA. The signals were injected into the PPLN module for OPA and idler waves were generated or signal-idler pairs were amplified. The 2-stage SHG/OPA configuration enables us to realize anoptical parametric process without the XT related to a high-power pump. This means that the 2-stage SHG/OPA-based PSA does not require a guard band for DWDM signals

Moreover, two different phase-matching bandwidths between the SHG and OPA process in PPLN enables the XT to be suppressed. The power of the SH-pump and idler waves is defined as [18]

$$P \propto \left[\frac{\sin\left(\Delta kL/2\right)}{\Delta kL/2}\right]^2 \left(\Delta k = \frac{n_3}{\lambda_3} - \frac{n_2}{\lambda_2} - \frac{n_1}{\lambda_1} - \frac{1}{\Lambda}\right) \quad (1)$$

where Δk is the phase mismatch, L is the length of the LN, n_1 is the refractive index at the signal light wavelength λ_1, n_2 is the refractive index at the converted light wavelength λ_2, n_3 is the refractive index at the pump light wavelength λ_3, and Λ is the poling period of PPLN. The calculated phase matching curves are shown in Fig. 2. In this calculation, we used the Sellmeier equation found in [19], and the parameters we employed were $L = 50$ mm, $\Lambda = 18.5\,\mu$m, and temperature $T = 50\,^{\circ}$C. The horizontal axis in Fig. 2(a) shows the SH-pump wavelength. In Fig. 2(b), the calculated DFG wavelength is shown on the horizontal axis when the signal at 776.5 nm is constant. The phase-matching bandwidth of OPA is very wide (about 60 nm), while the bandwidth of SHG is narrow (about 0.1 nm or 12.5 GHz at SH-band). Thanks to the fact that the SHG bandwidth is narrower than the DWDM channel spacing (typically ~50–100 GHz), we can suppress the XT using the undesired pump generated by the interaction between the signal-idler and the signal (or idler) itself.

We estimated the crosstalk experimentally using the setup shown in Fig. 3. 16-channel signals with a 100-GHz spacing (ITU Ch. C31 – C46) were generated with individual lasers and multiplexed with an arrayed waveguide grating (AWG). A 1553.33 nm (ITU Ch. C30) wave as a pump was input into one

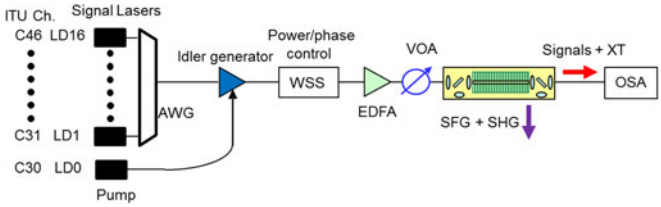

Fig. 3. Experimental setup for testing XT. Idler generator consists of 2-stage SHG/OPA configuration same as Fig. 1. AWG: arrayed waveguide grating, WSS: wavelength-selective switch, VOA: variable optical attenuator, EDFA: Er-doped fiber amplifier, OSA: optical spectrum analyzer.

second harmonic generator, and an SH-pump wave (776.67 nm) was generated. The pump and 16-channel signals were input into the PPLN waveguide to generate the phase conjugated idlers. After the idler generation, the power levels of the signal and the phase-conjugated idler pairs at the output of an EDFA were equalized with a difference of 1 dB for each channel by using a wavelength-selective switch (WSS). The signal and idler waves were amplified with an EDFA, input into a variable optical attenuator (VOA) to adjust the power level, and then input into an OPA module. The signal and idler waves were then converted to an SH-band pump through SHG or sum frequency generation (SFG) processes, which resulted in the generation of XT lights. The signal and idler waves were separated from the SH-band pump with the dichroic mirror, and detected with an optical spectrum analyzer (OSA).

Fig. 4(a) shows the output spectrum of the OPA module at an input power of 0 dBm/ch without C39 (1546.12 nm). XT induced by the nonlinear interaction between DWDM channels is clearly observed. The amount of XT changes when the input power level is adjusted. Fig. 4(b) shows the XT generated in three channels, 1540.56 nm (C46), 1551.72 nm (C32), and 1546.12 nm (C39). Note that a resolution bandwidth of 0.01 nm was set for this evaluation. We quantified the amount of XT as the power difference between the signal and the XT component. At an input power of less than −5 dBm/ch, the XT level curves of the three channels became nearly flat. This means that the XT components were near the noise floor level and negligibly small. We confirmed that the XT in the PPLN waveguide without the SH-pump (without a high power 1.5-μm-band pump) was negligible at an input power of less than −5 dBm/ch. These results indicate that we can expect low-crosstalk phase sensitive amplification in an OPA module in which the DWDM signal and SH-pump co-exist at an amplified signal level of less than −5 dBm/ch if the 1.5-μm-band pump and the accompanying ASE noise are sufficiently suppressed.

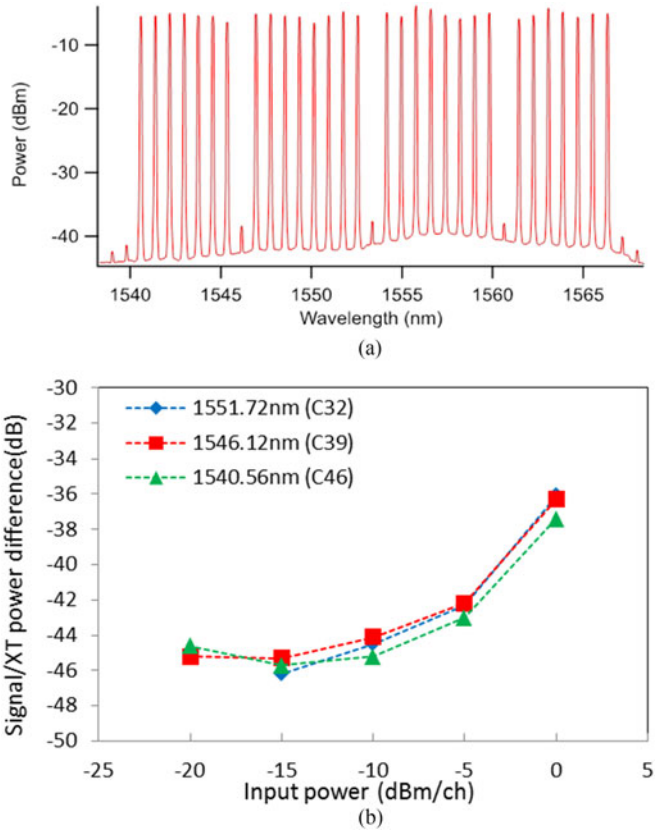

Fig. 4. XT estimation without SH-pump in OPA module. (a) Spectrum of OPA module output at input power of 0 dBm/ch without C39 (1546.12 nm), (b) measured XT levels for different channels. Three channels, 1551.72 nm (C32), 1546.12 nm (C39), and 1540.56 nm (C46), were measured with different input powers.

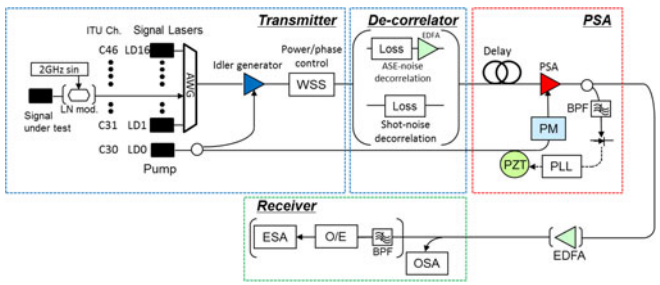

Fig. 5. Experimental setup for multi-channel PSA. The idler generator and PSA have a 2-stage SHG/OPA configuration as in Fig. 1. AWG: arrayed waveguide grating, WSS: wavelength-selective switch, PM: phase modulator, BPF: optical bandpass filter, PLL: phase-locked loop circuit, PZT: piezoelectric transducer, EDFA: erbium-doped fiber amplifier, OSA: optical spectrum analyzer, O/E: optical-electric converter, ESA: electrical spectrum analyzer.

III. Demonstration of Low XT Phase Sensitive Amplification for Guard-Band-Less DWDM Signals

Fig. 5 shows our experimental setup for a multi-channel PSA. The idler generator in the transmitter and the PSA have a 2-stage SHG/OPA configuration as in Fig. 1. The optical components noted in brackets are for evaluating the noise characteristics of the PSA as discussed in Section IV. At the transmitter, 16-channel signals with a 100-GHz spacing (ITU Ch. C31 – C46) and a pump at 1553.33 nm (ITU Ch. C30) were input into the idler generator. After the idler generation, the power levels of the signal and the phase-conjugated idler pairs were equalized with a very small difference of ±0.1 dB for each channel to obtain the optimum phase-sensitive characteristics with a WSS. Additionally, we adjusted the relative phase between the each signal-idler pair individually because of the simultaneous phase sensitive amplification of all the channels.

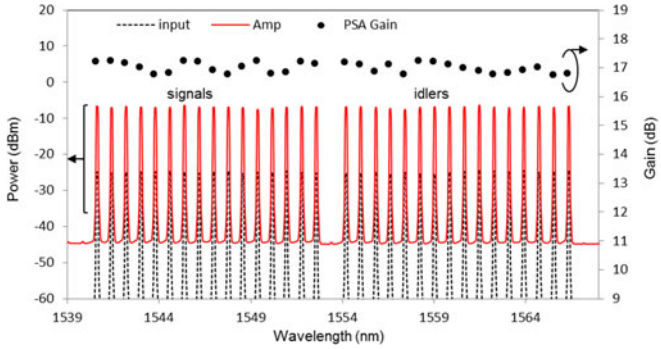

Fig. 6. PSA output spectra of 16-channel signal-idler pairs. The black line (only online) is the input spectrum and the red line (only online) is the output spectrum. The dots show the net gain of each channel.

Then, the signal-idler pair waves and the pump wave were injected into the PSA. The PSA output was tapped and filtered with an optical bandpass filter to detect interference between the signal and the corresponding idler waves. To achieve a stable PSA output, we used a piezoelectric transducer (PZT)-based phase-locked loop (PLL) to compensate for the slow relative phase drifts between the signal-idler pair and the SH-pump caused by temperature variations and acoustic vibrations. The bandwidth of the PLL circuit is a few tens of kHz, which is determined by the resonance frequency of the PZT device. At the receiver, the optical spectrum was measured with an OSA. To estimate the inter-channel XT, we compared the output spectra of the PSA with and without the signal under test.

Fig. 6 shows the optical spectra of the input signal-idler pairs and the PSA outputs at an input power of −25 dBm/ch. The dotted line is the input spectrum and the line is the amplified spectrum. On the other hand, the gain of each channel (right axis) is shown by the dots. The 16-channel signals were amplified simultaneously with an external gain of 17 dB. We obtained a flat gain of 17 ± 0.25 dB with a wide signal bandwidth of over 12 nm and without a guard band.

Fig. 7(a) shows the output spectra of the PSA with and without a signal wave C32 (at a wavelength of 1551.72 nm). We quantified the amount of XT based on the power difference between the amplified signal and an additionally induced converted signal at the same wavelength as the signal after subtracting the ASE noise level. A noise level of −46.2 dB by comparison with the amplified signal level was determined from the intrinsic ASE of the PSA because there was no ASE leakage from the EDFA in the pump to the OPA stage thanks to the high isolation of the pump. Fig. 7(b) shows the amount of XT as a function of the input power for different signal channels at the same PSA gain of 17 dB. We examined the XT for three different signals of the highest frequency, 2nd lowest frequency and middle frequency channels (1540.56 nm (C46), 1551.72 nm (C32), and 1546.12 nm (C39)). Although the XT for the middle frequency channel was slightly larger than those of the other channels, the XT for all three channels was clearly below the noise floor level of −46.2 dB at an input power less than −22.5 dBm/ch. These results show that a 2-stage SHG/OPA based PSA is tolerant to

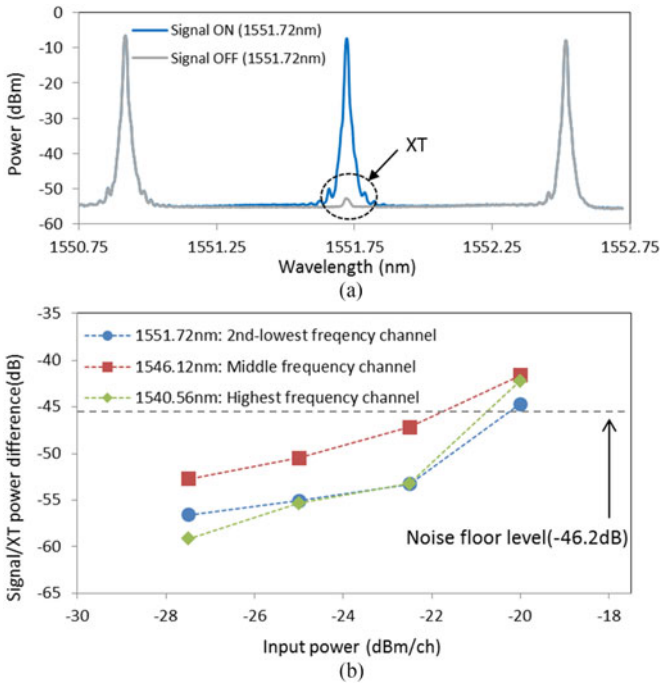

Fig. 7. Crosstalk estimation. (a) Output spectrum of PSA with and without 1551.72-nm signal, (b) measured XT level for different channels. Three channels, 1551.72 nm (C32), 1546.12 nm (C39), and 1540.56 nm (C46), were measured with different input powers.

the XT at an input power level below −22.5 dBm/ch, which is a feasible input power for a repeater amplifier used in DWDM signal transmission systems. We successfully demonstrated the simultaneous phase-sensitive amplification of guard-band-less 16-channel DWDM signals with a low XT.

IV. 16-Channel DWDM PSA With 3-dB Link SNR Improvement and Intrinsic Low NF Below 3-dB Quantum Limit

To evaluate the advantage of the PSA compared with a PIA such as an EDFA as regards both SNR improvement for a DWDM signal accompanied by ASE noise and an intrinsic low NF for a DWDM signal without the ASE, we captured the noise components in the electrical domain with an electrical spectrum analyzer (ESA) [20] as shown in Fig. 5. The signal under test was modulated using a Mach-Zehnder modulator with a 2-GHz sinusoidal wave to measure the amplifier gain in the electrical domain. We investigated the advantage of the SNR improvement by using a 16-channel input signal with ASE noise. Through idler generation, the noise under the signal-idler pair became fully correlated. To replace the correlated noise with uncorrelated ASE noise, we inserted a large loss of 25 dB and amplification with an additional EDFA, which emulated the link loss and a repeater amplifier. Fig. 8 shows the output noise power densities of the signal under test for a 16-channel signal input and a single-channel signal input as a function of the input power. As a reference, we also plotted the results when the 16-channel signal was amplified by another EDFA with the same gain of 17 dB. We observed an average 2.5 dB SNR improvement

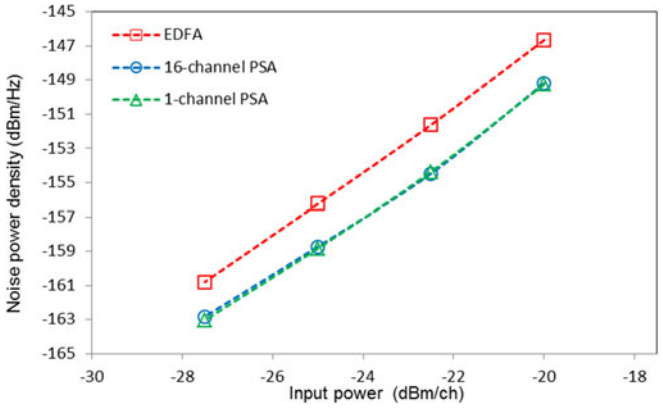

Fig. 8. Noise level of 16-channel PSA, single-channel PSA and EDFA. The test channel is C32.

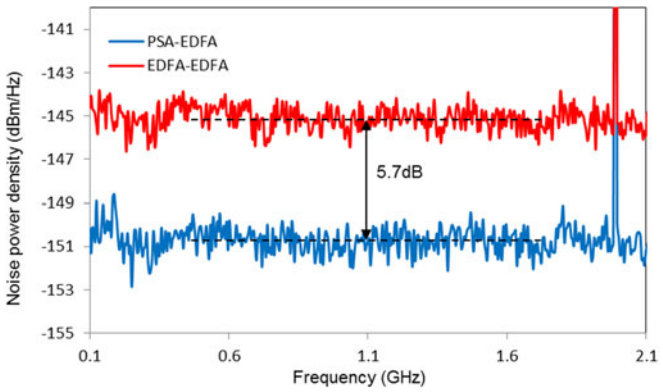

Fig. 9. Electrical noise spectra of EDFA-EDFA cascade amplifier and PSA-EDFA cascade amplifier. Resolution bandwidth is 1 MHz. The peak at 2 GHz is caused by intensity modulation.

with the PSA by comparison with the EDFA. The nearly 3-dB SNR improvement compared with uncorrelated ASE noise resulted from the additional coherent gain for the signal. Almost the same noise level within a difference of −0.1 dB was obtained between the 16-channel and single-channel PSAs, which means that the effect of the XT was negligibly small.

Then, we examined the intrinsic NF of the PSA by comparing a reference EDFA. The external gain of the reference EDFA was 17 dB as was the gain of the PSA. In this experiment, only a large loss of 25 dB was added for noise decorrelation. The correlated noise in the signal-idler pairs was replaced with shot noise. To mitigate the narrow dynamic range of the ESA, we cascaded the PSA with an EDFA. The cascaded EDFA had an external gain of 15 dB and an NF of 4.8, which was measured with an OSA [20]. We measured the output noise power density for the PSA-EDFA amplifiers and for EDFA-EDFA amplifiers. Fig. 9 shows the electrical noise spectra of C32 in the 0.1 to 2-GHz range for both amplifiers under the same signal input power condition of −35 dBm/ch. The PSA-EDFA amplifier exhibited a 5.7 dB smaller noise power than the EDFA-EDFA amplifier. We calculated the NF value of the PSA using the NF values of the EDFAs measured with the OSA. The measured

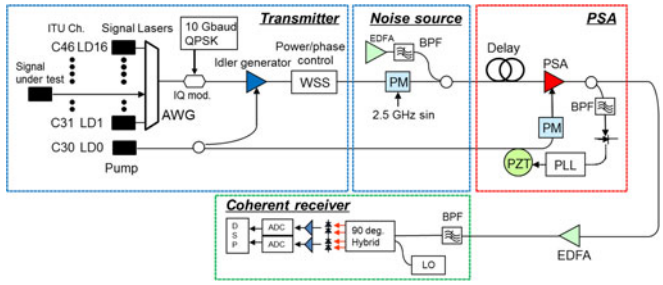

Fig. 10. Experimental setup for multi-channel PSA. Idler generator and PSA with a 2-stage SHG/OPA configuration as in Fig. 1. AWG: arrayed waveguide grating, WSS: wavelength-selective switch, PM: phase modulator, BPF: optical bandpass filter, PLL: phase-locked loop circuit, PZT: piezoelectric transducer, EDFA: erbium-doped fiber amplifier, OSA: optical spectrum analyzer, LO: local oscillator, ADC: analog to digital converter, DSP: digital signal processing.

NF of the EDFA-EDFA amplifier used for the reference was 5.0 dB. From the noise level difference of 5.7 dB, we determined that the NF of the PSA-EDFA amplifier was −0.7 dB. If we assume that the output noise is dominated by the beat noise between the ASE noise and the amplified signal and the shot noise of the amplified signal, the NF of a cascaded PSA and EDFA can be expressed by following equation [20],

$$F_{\mathrm{PSA+EDFA}} = F_{\mathrm{PSA}} + \frac{F_{\mathrm{EDFA}} - 1}{G_{\mathrm{PSA}}} \tag{2}$$

where G_{PSA} is the gain of the PSA, and F_{PSA} and F_{EDFA} are the NFs of the PSA and EDFA, respectively. Using Eq. (2) to evaluate the NF of the PSA from the measured NF of the PSA-EDFA and the cascaded EDFA, we found that the value was −0.9 dB, which is the separate NF of the PSA when we consider each signal and idler individually. The combined NF is a more general and reasonable definition of NF for non-degenerate PSAs because both signal and idler are present at the input and carry the same information [14]. When we take account of the combined input powers, which would lead to a 3 dB higher input SNR, the combined NF of the PSA corresponded to 2.1 dB. We confirmed that the PSA exhibited an SNR advantage of about 6 dB and a low NF below the 3-dB quantum limit compared with the EDFA.

V. QPSK Signals Amplification With Phase and Amplitude Regeneration

Finally, we demonstrated QPSK demodulation after the PSA. To confirm the signal regeneration property of the PSA, we evaluated the Q-factors for a single polarized QPSK signal using the experimental setup shown in Fig. 10. The transmitter generated a 10-Gbaud QPSK signal at ITU Ch. C31 to C46. Phase-conjugated idlers were generated as described in Sections II and III to achieve the non-degenerated phase sensitive amplification of the QPSK signal. A $LiNbO_3$ phase modulator was used to add phase distortion and an EDFA was used to add ASE noise. Signal-idler pairs with phase distortion or ASE noise were input into the PSA at an input power of −20 dBm/ch. After the PSA, the QPSK signals were detected by a digital coherent receiver with offline processing.

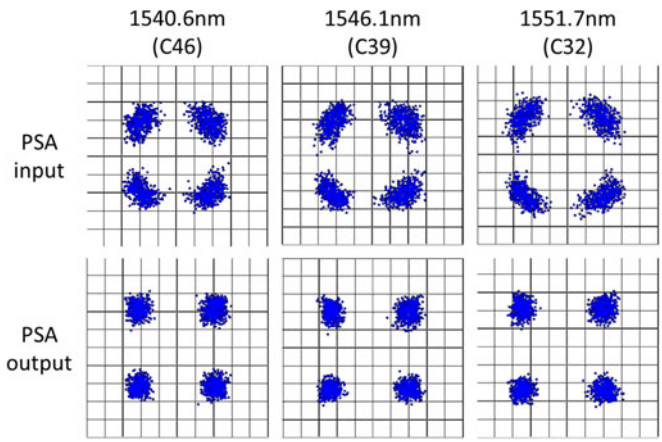

Fig. 11. Constellation diagrams of input signals with phase distortion and the output signals at C32, C39, and C46 after the PSA.

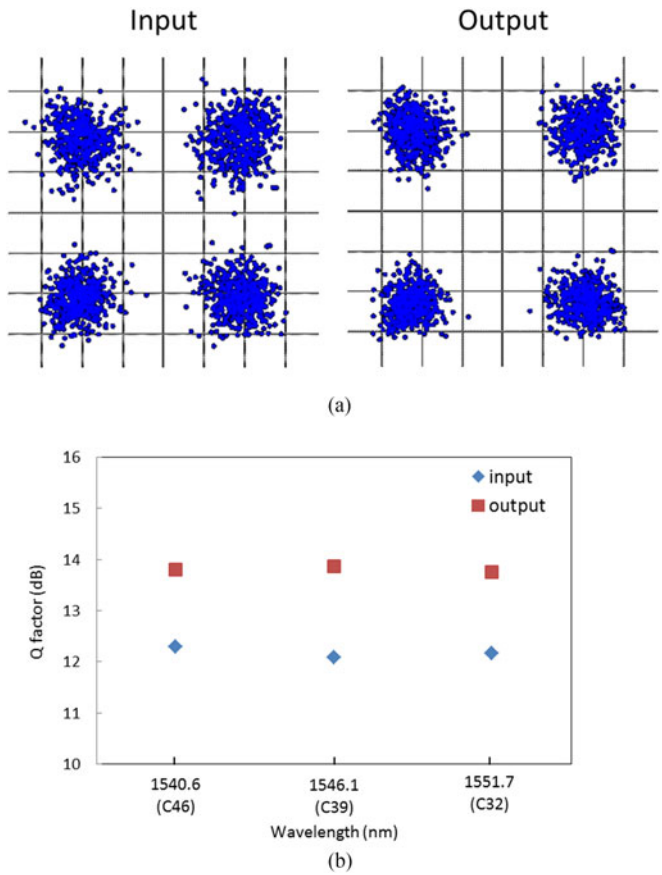

Fig. 12. Q-factors at the PSA input and output and constellation diagrams. (a) Constellation diagrams of the PSA input and output. The test signal is ITU Ch. C39. (b) Q-factors at the PSA input and output.

Fig. 11 shows constellation diagrams for a 10-Gb/s QPSK input signals with phase distortion and the output signals at C32, C39, and C46 after the PSA. The phase modulator was driven at a frequency of 2.5 GHz to introduce a sinusoidal phase variation. As shown in the constellation of the input signals, the constellation points were rotationally spread due to the phase distortion. The Q-factors for three channel input signals at C32, C39, and C46 were 11.8, 12.1, and 12.1 dB, respectively. In this phase distortion emulation setup, the same phase variation was added to both signal and idler, namely $\phi_{\rm signal}+\delta\phi$ and $\phi_{\rm idler}+\delta\phi = -\phi_{\rm signal}+\delta\phi$. At the PSA, the idler generates a phase conjugated signal, namely $-(\phi_{\rm idler}+\delta\phi = \phi_{\rm signal}-\delta\phi$. As a result, the phase noise will be canceled by using the phase conjugated idler. After the PSA, a major phase distrotion reduction was achieved by the canceling effect. The Q-factors for the PSA output signals at C32, C39, and C46 were 16.4, 16.7, and 16.4 dB, respectively. We confirmed signal restoration after the PSA.

Fig. 12(a) shows the constellation of the input signal with ASE noise and the output signal at C39. The OSNR of the input signal was 15 dB. After applying the PSA, a clearly recovered constellation diagram was obtained thanks to the advantage of the improved SNR of the non-degenerate PSA. Fig. 12(b) shows the Q-factors at C32, C39, and C46. The Q-factors of the three channel signals improved by about 1.5 dB. These results show that the PSA simultaneously amplifies DWDM-QPSK signals with phase and amplitude noise reduction. Although, we used only a single polarization signal in this experiment, PDM signal amplification is also possible by using a polarization-diversity configuration [21].

VI. Conclusion

We realized a low-XT PSA for DWDM signal amplification without a guard band using a 2-stage SHG/OPA configuration. The 2-stage PPLN-based configuration enabled the mitigation of the parametric XT generation related to a strong telecom-band pump. We demonstrated the simultaneous phase-sensitive amplification of 16-channel CW-signals with a high gain of 17 dB over a 12-nm wavelength range. Thanks to the 2-stage configuration, the amount of XT was negligibly small in the PSA at a feasible input power for a repeater amplifier. The PSA provided a 2.5-dB link SNR advantage over an EDFA because of the gain difference between the signal and the noise and a low combined NF below the 3-dB quantum limit. The amplification of a 10-Gbaud DWDM QPSK signal was achieved with phase and amplitude regeneration. These results indicate that the PSA will be useful as a repeater amplifier for the spectrally efficient large capacity photonic networks of the future.

Acknowledgment

Part of this research uses results of the "R&D on Optical Signal Transmission and Amplification with Frequency/Phase Precisely Controlled Carrier" commissioned by the National Institute of Information and Communications Technology of Japan.

References

[1] R. Essiambre and R. W. Tkach, "Capacity trends and limits of optical communication networks," *Proc. IEEE*, vol. 100, no. 5, pp. 1035–1055, May 2012.

[2] C. M. Caves, "Quantum limits on noise in linear amplifiers," *Phys. Rev. D*, vol. 26, no. 8, pp. 1817–1839, Aug. 1982.

[3] K. Croussore and G. Li, "Phase regeneration of NRZ-DPSK signals based on symmetric-pump phase-sensitive amplification," *IEEE Photon. Technol. Lett.*, vol. 19, no. 11, pp. 864–866, Jun. 2007.
[4] W. Imajuku, A. Takada, and Y. Yamabayashi, "Low-noise amplification under the 3-dB noise figure in a high gain phase-sensitive fiber amplifier," *Electron. Lett.*, vol. 35, no. 22, pp. 1954–1955, 1999.
[5] T. Umeki, O. Tadanaga, A. Takada, and M. Asobe, "Phase sensitive degenerate parametric amplification using directly-bonded PPLN ridge waveguides," *Opt. Express,* vol. 19, no. 7, pp. 6326–6332, 2011.
[6] C. J. McKinstrie and S. Radic, "Phase-sensitive amplification in a fiber," *Opt. Express*, vol. 20, no. 20, pp. 4973–4979, Oct. 2004.
[7] B. J. Puttnam, D. Mazroa, S. Shinada, and N. Wada, "Phase-squeezing properties of non-degenerate PSAs using PPLN waveguides," *Opt. Express*, vol. 19, no. 26, pp. B131–B139, 2011.
[8] Z. Tong, C. Lundström, E. Tipsuwannakul, M. Karlsson, and P. A. Andrekson, "Phase-sensitive amplified DWDM DQPSK signals using free-running Lasers with 6-dB link SNR improvement over EDFA-based systems," presented at the *Eur. Conf. and Exhibition on Optical Communication*, Torino, Italy, 2010, Paper PDP1.3.
[9] B. J. Puttnam, A. Szabo, D. Mazroa, S. Shinada, and N. Wada, "Multichannel phase squeezing in a PPLN-PPLN PSA," presented at the *Optical Fiber Commun. Conf.*, Los Angeles, CA, USA, 2012, Paper OW3C.6.
[10] R. Tang *et al.*, "Gain characteristics of a frequency nondegenerate phase-sensitive fiberoptic parametric amplifier with phase self-stabilized input," *Opt. Express*, vol. 13, no. 26, pp. 10483–10493, Dec. 2005.
[11] Z. Tong *et al.*, "Modeling and measurement of noise figure in a cascaded non-degenerate phase-sensitive parametric amplifier," *Opt. Express*, vol. 18, no. 14, pp. 14820–14835, Jul. 2010.
[12] M. Vasilyev, "Phase-sensitive amplification in optical fibers," presented at the *Frontiers in Optics, Technical Digest Series*, Tucson, AZ, USA, 2005, Paper FThB1.
[13] P. L. Voss, K. G. Köprulu, and P. Kumar, "Raman-noise-induced quantum limits for $\chi(3)$ nondegenerate phase-sensitive amplification and quadrature squeezing," *J. Opt. Soc. Amer. B*, vol. 23, no. 4, pp. 598–610, Apr. 2006.
[14] Z. Tong, C. Lundström, P. A. Andrekson, M. Karlsson, and A. Bogris, "Ultralow noise, broadband phase-sensitive optical amplifiers, and their applications," *IEEE J. Sel. Topics. Quantum Electron.*, vol. 18, no. 2, pp. 1016–1032, Mar./Apr. 2012.
[15] Á. Szabó *et al.*, "Numerical comparison of WDM interchannel crosstalk in FOPA- and PPLN-based PSAs," *IEEE Photon. Technol. Lett.*, vol. 26, no. 15, pp. 1503–1506, Aug. 2014.
[16] T. Kazama *et al.*, "Low-noise phase-sensitive amplifier for guard-bandless 16-channel DWDM signal using PPLN waveguides," presented at the *Optical Fiber Conf.*, Anaheim, 2016, Paper M3D.1.
[17] T. Umeki, O. Tadanaga, and M. Asobe, "Highly efficient wavelength converter using direct-bonded PPZnLN ridge waveguide," *IEEE J. Quantum Electron.*, vol. 46, no. 8, pp. 1206–1213, Aug. 2010.
[18] T. Yanagawa *et al.*, "Simultaneous observation of co isotopomer absorption by broadband difference-frequency generation using a direct-bonded quasi-phase-matched linbo3 waveguide," *Opt. Lett.*, vol. 31, no. 7, pp. 960–962, Apr. 2006.
[19] D. H. Jundt, "Temperature-dependent Sellmeier equation for the index of refraction, ne, in congruent lithium niobate," *Opt. Lett.*, vol. 22, no. 20, pp. 1553–1555, Oct. 1997.
[20] M. Asobe, T. Umeki, and O. Tadanaga, "Phase sensitive amplification with noise figure below the 3 dB quantum limit using CW pumped PPLN waveguide," *Opt. Express*, vol. 20, pp. 13164–13172, Jun. 2012.
[21] T. Umeki *et al.*, "PDM signal amplification using PPLN based polarization-independent phase-sensitive amplifier," *J. Lightw. Technol.*, vol. 33, no. 7, pp. 1326–1332, 2015.

Takushi Kazama received the B.S. and M.S. degrees in electrical engineering from the University of Tokyo, Tokyo, Japan, in 2009 and 2011, respectively. In 2011, he joined the NTT Photonics Laboratories (later reorganized into NTT Device Technology Laboratories), Atsugi-shi, Japan, where since then he has been involved in research on periodically poled lithium niobate waveguide devices. He is a Member of the Institute of Electronics, Information, and Communication Engineers of Japan and the Japan Society of Applied Physics.

Takeshi Umeki received the B.S. degree in physics from Gakusyuin University, Tokyo, Japan, in 2002, and the M.S. degree in physics and the Ph.D. degree in the area of nonlinear optics from the University of Tokyo, Tokyo, in 2004 and 2014, respectively. He joined the NTT Photonics Laboratories (later reorganized into NTT Device Technology Laboratories), Atsugi-shi, Japan, in 2004, since then he has been involved in research on nonlinear optical devices based on periodically poled $LiNbO_3$ waveguides. He is a Member of the Japan Society of Applied Physics and the Institute of Electronics, Information, and Communication Engineers.

Masashi Abe received the B.S. and M.S. degrees in physics and the Ph.D. degree in the area of quantum electronics from Keio University, Kanagawa, Japan, in 2006, 2008, and 2015, respectively. In 2015, he joined the NTT Device Technology Laboratories, Atsugi-shi, Japan, where he has been involved in research on the application of periodically poled lithium niobate waveguide devices. He is a Member of the Physical Society of Japan.

Koji Enbutsu received the B.E. and M.E. degrees in electronics engineering from Hokkaido University, Sapporo, Japan, in 1994 and 1996, respectively. In 1996, he joined NTT Opto-electronics Laboratories, Ibaraki, Japan, where he was engaged in research on organic optical waveguides for optical communications and electro-optic crystals and their devices. In 2007, he moved to NTT Access Services Network System Laboratories, Atsugi-shi, Japan, where since then he has been focusing on research on optical fiber testing and monitoring. He is a Member of the Institute of Electronics, Information and Communication Engineers and the Japan Society of Applied Physics.

Yutaka Miyamoto (M'93) received the B.E. and M.E. degrees in electrical engineering from Waseda University, Tokyo, Japan, in 1986 and 1988, respectively. In 1988, he joined the NTT Transmission Systems Laboratories, Yokosuka, Japan, where he was involved in research and development on high-speed optical communications systems including the 10-Gb/s first terrestrial optical transmission system (FA-10G) using EDFA inline repeaters. He then joined the NTT Electronics Technology Corporation between 1995 and 1997, where he was involved in the planning and product development of high-speed optical module at the data rate of 10 Gb/s and beyond. Since 1997, he has been with the NTT Network Innovation Laboratories, Yokosuka, where he has contributed in the research and development of optical transport technologies based on 40/100-Gb/s optical channels. He is currently the Director of Innovative Photonic Network Research Center, NTT Network Innovation Laboratories, where he has been investigating and promoting the scalable optical transport network with the Pbit/s-class capacity based on innovative transport technologies such as digital signal processing, space division multiplexing, and cutting-edge integrated devices for photonic pre-processing. He is currently the Director for *Journal and Transactions of IEICE*, and the Vice-Chair of the IEICE study group of Extremely Advanced Optical Transmission. He is a Senior Distinguished Researcher at the NTT Laboratories and a Fellow of IEICE.

Hirokazu Takenouchi (M'14) received the B.S. and M.S. degrees in pure and applied sciences from the University of Tokyo, Tokyo, Japan, in 1992 and 1994, respectively, and the Ph.D. degree in ultrafast optical signal processing from the Tokyo University of Agriculture and Technology, Tokyo, in 2005. In 1994, he joined the NTT Optoelectronics Laboratories, Atsugi-shi, Japan, where he was involved in research on such areas as optical signal processing for high-capacity optical transport networks. He is currently a Leader of the Optoelectronic Subsystem Research Group, NTT Device Technology Laboratories, Atsugi-shi, Japan, and is a Senior Research Engineer, Supervisor at the Innovative Photonic Network Center, NTT Network Innovation Laboratories, Yokosuka, Japan. He is a Member of the Japan Society of Applied Physics and a Senior Member of the Institute of Electronics, Information, and Communication Engineers.